

TrajTok: Learning Trajectory Tokens Enhances Video Understanding

Chen hao Zheng^{1,2}, Jieyu Zhang^{1,2}, Jianing Zhang¹, Weikai Huang^{1,2}, Ashutosh Kumar⁴, Quan Kong⁴, Oncel Tuzel³, Chun-Liang Li³, Ranjay Krishna^{1,2}

¹University of Washington, ²Allen Institute for Artificial Intelligence, ³Apple, ⁴Woven by Toyota, Inc

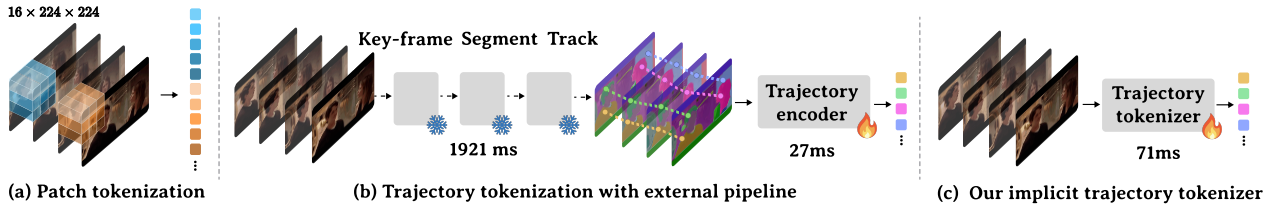


Figure 1. (a) Traditional video tokenization splits a video into space-time patches, introducing large number of redundant tokens. (b) Prior work [84] proposes to represent a video via panoptic sub-object trajectory, which significantly reduces redundancy but relies on slow, non-differentiable pipelines. (c) we propose TrajTok, an end-to-end differentiable trajectory tokenizer that learns to implicitly propose trajectory tokens, offering low token counts, efficiency and adaptability to downstream objectives.

Abstract

Tokenization in video models, typically through patchification, generates an excessive and redundant number of tokens. This severely limits video efficiency and scalability. While the recent trajectory-based tokenizers offer a promising solution by decoupling video duration from token count, they rely on complex, external segmentation and tracking pipelines that are slow and task-agnostic. We propose **TrajTok**, an end-to-end video tokenizer module that is fully integrated and co-trained with video models for a downstream objective, dynamically adapting its token granularity to semantic complexity, independent of video duration. TrajTok contains a unified segmenter that performs implicit clustering over pixels in both space and time to directly produce object trajectories in a single forward pass. By prioritizing downstream adaptability over pixel-perfect segmentation fidelity, TrajTok is lightweight, efficient, and yet empirically improves video understanding performance. With TrajTok, we implement a video CLIP model trained from scratch (**TrajViT2**). It achieves the best accuracy at scale across both classification and retrieval benchmarks, while maintaining efficiency comparable to the best token-merging methods. TrajTok also proves to be a versatile component beyond its role as a tokenizer. We show that it can be seamlessly integrated as either a probing head for pretrained visual features (**TrajAdapter**) or an alignment connector in vision-language models (**TrajVLM**) with especially strong performance in long-video reasoning.

1. Introduction

Now that transformers are the dominant backbone in modern computer vision, designing effective tokenizers for visual inputs is a central research question [5]. Tokenization for videos is particularly challenging due to their long duration and large number of near-duplicate frames. Today’s de-facto tokenization algorithms split the video tensor into space-time patches (Figure 1(a)). Whether training a ViT directly on raw video frames [1, 4, 72], adapting a pretrained vision encoder’s representations for downstream tasks [2, 3], or feeding visual tokens into a large vision-language model [17, 54], visual tokens are almost invariably represented as regular grids of patches. However, this fixed and spatially uniform tokenization becomes increasingly inefficient as the resolution or length of the video grows, leading to severe memory bottlenecks [1].

Tokenization in video models, typically via simple patchification, produces an excessive number of spatio-temporal tokens, significantly limiting efficiency and scale. Recent token reduction efforts, which group semantically similar regions, often fail either by requiring predefined token counts [6, 14, 48], preventing adaptation to input complexity [58]; or by compromising robustness due to sensitivity to scene motion [6, 14, 15]. A more compelling alternative, TrajViT [84] introduced a promising paradigm by treating sub-object trajectories as the fundamental unit of video tokenization (Figure 1(b)). Trajectory-based tokenization effectively decouples video duration from the total token count, and, for the first time, demonstrates that tokens after grouping outperform raw patch tokens on all

downstream tasks. However, this approach is fundamentally limited by its reliance on using external task-agnostic segmentation and tracking models [10, 57] to generate object trajectories, making the tokenizer a slow, independent, non-trainable preprocessing step.

We believe in the potential of organizing visual tokens according to object trajectories, as it closely aligns with human perceptual principles [53, 62, 66]; yet, we argue relying on an external pipeline to generate these trajectories is suboptimal. Not only does it reduce efficiency and introduce longer latency, but it fixes the semantic granularity of the token unit using general-purpose segmentation models that may not be optimal for the downstream task. For instance, in understanding a particular dance performance, a model might require tokens representing dancers’ individual body parts for fine-grained movements, whereas the task of identifying group formations might benefit from representing each dancer as a single, unified token. This mismatch motivates our goal: to build an implicit trajectory video tokenizer where the trajectory-generation module is seamlessly integrated into and co-trained with the rest of the network in an end-to-end manner, fully supervised by the downstream objective.

We present **TrajTok**, an end-to-end video tokenizer that learns to group trajectories and proposes implicit trajectory tokens. TrajTok is much more efficient than prior work [84] and is not rigid; it adapts its tokenization to the downstream tasks (Figure 1(c)). Much of the compute in modern segmentation and tracking models is devoted to achieving pixel-perfect masks [12, 31, 79, 80], which is often superfluous for high-level understanding tasks. By contrast, TrajTok trades off pixel-perfect accuracy with end-task performance. This is achieved by formulating trajectory generation as an implicit clustering problem over input pixels—both in space and in time. By treating spatial and temporal dimensions uniformly, we design a unified segmenter that processes an entire video in one forward pass to directly output clusters of object trajectories. Empirically, we show that reduced segmentation accuracy doesn’t harm and instead improves understanding performance. Finally, our trajectory encoder incorporates adaptive representation inspired by Matryoshka [34], enabling adaptive token number per trajectory and resolving the issue of over-compressed representations for objects undergoing complex or articulated motion.

With TrajTok, we train **TrajViT2**, a transformer encoder from scratch using the CLIP objective [55], and evaluate it on classification and retrieval benchmarks. Our approach achieves the best accuracy across both classification and retrieval benchmarks, including a large-margin improvement of +4.8% on Kinetics-400 and +4.1% on SSV2 over a standard video ViT, while being as efficient in inference FLOPs when compared against state-of-the-art token-

merging methods [6, 14, 15]. Furthermore, we observe better scaling trends than TrajViT [84] as training-dataset size increases, possibly because of our segmenter’s flexibility in adapting to downstream tasks (Figure 3).

TrajTok is versatile and more than just a tokenizer. We show that a pretrained TrajTok can also be used in two other scenarios. First, we design **TrajAdapter** as a feature adapter, inserted after a pretrained ViT. We show TrajAdapter provides a cost-effective way to enhance the probing performance of pretrained encoders in common video classification benchmarks without full fine-tuning. Second, we design **TrajVLM**, a vision-language model with TrajTok as the alignment module. When positioned between a ViT and an LLM, TrajTok improves video question-answering performance, especially for long-video questioning benchmarks. Together, these results highlight the potential of our end-to-end trajectory tokenizer as a unified, efficient, and semantically grounded tokenization module for dozens of video understanding tasks.

2. Related work

Video tokenization and efficient video encoders. Modern video transformers initially adopted fixed space-time patches [1, 4, 43], but this leads to high token counts and heavy compute. To address this, a broad range of techniques has emerged, including token pruning and merging [6, 13, 14, 19, 29, 36, 56, 67], latent-bottleneck or learned-token approaches [26, 27, 50, 58], and recent online or large-context video-LLM systems [25, 40, 73, 77]. A persistent challenge across these efficiency-oriented designs is that their performance often lags behind patch-based tokenization, and scaling them to larger datasets or architectures remains difficult. More recently, trajectory-centric tokenization [84] has shown that organizing tokens by visual trajectories can simultaneously improve accuracy and reduce token counts.

Object-centric representations. Object-centric learning has long aimed to represent scenes as compositions of discrete entities rather than unstructured patches. Early slot-based and scene decomposition models demonstrated the benefits of learning object-level structure from raw visual inputs [7, 24, 30, 44, 61]. Foundation segmentation models such as SAM and SAM2 [31, 57] further enable region-level visual abstractions that improve grounding in vision-language models like Osprey [82]. In the context of video representation, both TrajViT [84] and Trokens [33] extend this object-centric perspective by introducing semantic, trajectory-based tokenization that groups spatio-temporal features into object-consistent units. Our work builds on this insight, generalizing trajectory-based tokenization into an end-to-end differentiable framework.

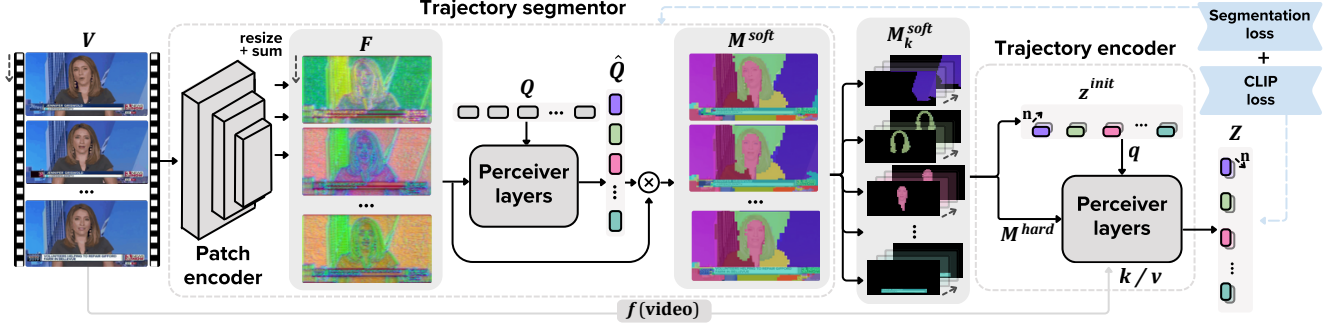


Figure 2. **Overview of the TrajTok architecture.** TrajTok comprises a *trajectory segmenter* and a *trajectory encoder*. The segmenter proposes trajectory masks for all objects in an image or video within a single forward pass. The encoder then aggregates raw video pixels or encoded visual features (parameterized by f in the figure) according to these masks to produce trajectory tokens. The number of tokens per trajectory can be flexibly adjusted based on the available compute budget.



Figure 3. **Training with downstream understanding tasks reshapes the segmentation granularity.** We visualize the trajectory masks produced by our segmenter when trained with only segmentation supervision versus jointly with segmentation and CLIP objectives. The CLIP objective reshapes the segmentation granularity, producing finer foreground object masks while merging background regions.

3. TrajTok

We aim to design an end-to-end, efficient, and semantically grounded tokenizer that converts visual inputs (images or videos) into a compact set of tokens representing object trajectories. Let $\mathbf{V} \in \mathbb{R}^{T \times H \times W \times 3}$ denote an input video with T frames and spatial resolution $H \times W$. Our goal is to learn a mapping $\mathcal{T} : \mathbf{V} \rightarrow \mathbf{Z}$, where $\mathbf{Z} \in \mathbb{R}^{N \times d}$ is a set of N trajectory tokens with dimension d . N is not fixed and depends on semantic complexity of the video.

The tokenizer consists of two differentiable components, which were trained jointly: a *universal segmenter* that partitions the input into semantic groups, and a *trajectory encoder* that aggregates these groups into compact latent tokens. We visualize the architecture in Figure 2.

3.1. Universal segmenter for trajectory grouping

The segmenter is a lightweight and efficient module that performs effective semantic grouping in a single feedforward pass. It decouples video duration from the final token count. We value robust semantic grouping over pixel-perfect segmentation masks, and design a simple and efficient module to achieve this.

Frame-wise feature extraction. We first extract a high-resolution feature map from \mathbf{V} using a lightweight patch encoder. We use ConvNeXt [42] architecture as it naturally provides multi-scale feature maps. We extract features

frame-wise. Multi-scale maps are resized to their highest resolution ($1/4$ of original image size) and summed to form the final dense feature representation $\mathbf{F} \in \mathbb{R}^{T \times h \times w \times d}$, where $h, w = H/4, W/4$.

Learnable queries for semantic grouping. We introduce a set of N_q learnable latent queries $\mathbf{Q} \in \mathbb{R}^{N_q \times d}$ that act as cluster prototypes. These queries are processed through a stack of Perceiver [26] layers. Within each perceiver layer, queries \mathbf{Q} attend to the dense features \mathbf{F} using cross-attention. To handle inputs with variable frame counts T and encode spatiotemporal structure, we apply 1D Rotary Positional Embeddings (RoPE) [63] to the patch features \mathbf{F} before attention. The resulting processed queries, $\hat{\mathbf{Q}} = \text{Perceiver}(\mathbf{Q}, \text{RoPE}(\mathbf{F}))$, encapsulate the semantic information necessary for segmentation.

Soft segmentation. We generate segmentation masks by computing the similarity between processed queries and patch features. A soft segmentation map $\mathbf{M}^{\text{soft}} \in [0, 1]^{N_q \times T \times h \times w}$ is obtained via softmax over the query dimension of the dot-product similarity:

$$\mathbf{M}_{k,t,i,j}^{\text{soft}} = \text{softmax}_k(\hat{\mathbf{q}}_k \cdot \mathbf{F}_{t,i,j}) \quad (1)$$

where $\hat{\mathbf{q}}_k$ is the k -th processed query and $\mathbf{F}_{t,i,j}$ is the feature at time t and spatial location (i, j) . We find that feature maps at $1/4$ resolution provide sufficient detail for grouping, obviating the need for any compute-heavy decoders used in off-the-shelf segmenters [12, 81]. Furthermore, we

detach the gradients of \mathbf{F} before entering the Perceiver layers to prevent unstable co-adaptation between patch features and learnable queries.

While the number of learnable queries N_q is fixed, the number of trajectories N can vary. Queries that produce empty masks are discarded, and long videos are divided into temporal chunks that can be processed in parallel. This mechanism allows the tokenizer to propose a dynamic number of tokens that scales naturally with scene complexity.

Training the segmenter. The segmenter can be trained either independently or jointly with the other objectives. We use supervised learning for the segmenter with pseudo ground-truth masks (generated via the TrajViT [84] pipeline). We find that a combination of *Dice loss* [64] and *Focal loss* [38], without standard *cross-entropy*, yields the best downstream understanding. This combination prioritizes the discovery of all object regions over strict pixel-level class accuracy. This recipe likely arises because pixel-level precision is less critical for the downstream video benchmarks and applications we evaluate. In particular, Dice loss plays a central role in the discovery of all object regions within the visual input, ensuring robust semantic grouping.

3.2. Trajectory encoder

The trajectory encoder aggregates patch-level feature maps into compact tokens corresponding to segmented regions. Unlike prior approach [84], our encoder accepts both soft and hard segmentations to ensure differentiability while maintaining disentangled representations. We default to use the patch encoder’s features F as the input feature map, but in practice it can be provided by any pretrained feature $f(\text{video})$, enabling our tokenizer to operate as a plug-in feature adapter across diverse downstream tasks.

Trajectory proposal generation. Initial trajectory embeddings are generated by a weighted aggregation of features using the soft masks. The proposal embedding $\mathbf{z}_k^{\text{init}}$ for the k -th trajectory is computed as:

$$\mathbf{z}_k^{\text{init}} = \sum_{t,i,j} \mathbf{M}_{k,t,i,j}^{\text{soft}} \cdot \mathbf{F}_{t,i,j} \quad (2)$$

This soft aggregation allows gradients from downstream tasks to flow back into the segmenter. However, weighted summing can lead to information loss and blurred representations, which we address next.

Trajectory embedding refinement. To sharpen these representations, we employ a second Perceiver module. The initial proposals \mathbf{z}^{init} serve as cluster representations. We can now use them as queries to extract meaningful representations from \mathbf{F} . To ensure disentanglement, we enforce *masked* cross-attention using hard segmentation maps, \mathbf{M}^{hard} , obtained by applying an argmax to \mathbf{M}^{soft} and converting to one-hot binary assignments. The k -th query $\mathbf{z}_k^{\text{init}}$ is only allowed to attend to features $\mathbf{F}_{t,i,j}$ where

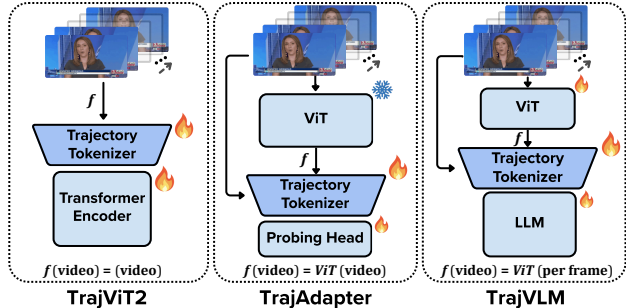


Figure 4. **TrajTok is a versatile module applicable across pre-training, feature adaptation, and finetuning stages.** We demonstrate its use in three scenarios: TrajViT2, which trains a visual encoder from scratch; TrajAdapter, which adapts pretrained features for downstream tasks; and TrajVLM, which uses TrajTok as a connector in LLaVA-style large vision–language models.

$\mathbf{M}_{k,t,i,j}^{\text{hard}} = 1$. This refinement recovers fine-grained motion and texture details specific to the trajectory’s region.

Adaptive token number per trajectory. In practice, assigning a single token to each trajectory can be overly restrictive, especially for trajectories that span long durations, exhibit complex motion, or undergo substantial appearance changes. We introduce an adaptive token mechanism inspired by Matryoshka representations [34] to balance efficiency and expressivity. Given a predefined compute budget, the encoder can emit $n \in \{1, 2, 4\}$ tokens per trajectory, enabling a flexible trade-off between efficiency and expressivity. This mechanism is applied during the Trajectory embedding refinement, where each trajectory token can be expanded into multiple sub-tokens. We illustrate the details next.

For each of the initial trajectory embedding $\mathbf{z}_k^{\text{init}}$, we duplicate the token n times and associate each copy with a distinct learnable query vector. During the subsequent attention step, these queries interact with the same set of patch features, allowing them to capture complementary aspects of the same trajectory. However, we observe minimal performance gain with a naive initialization of these queries, as they tend to attend to the same dominant regions without explicit encouragement of diversity. To encourage diversity among sub-tokens, these queries are initialized with Fourier positional embeddings with angular offsets that maximally separate them in feature space.

To train such tokens, similar to Matryoshka Representations, we randomly sample $n \in \{1, 2, 4\}$ for each batch during training so that a single model can handle multiple token granularities. At inference, n can be adjusted according to available computational resources.

4. Experiments

In our experiments, we demonstrate that **TrajTok** is a high-performance, efficient, and widely applicable module. It

can operate directly on raw video pixels to propose trajectory tokens, or act as a feature adapter module applied to pretrained vision features.

We evaluate TrajTok in three distinct scenarios, shown in Figure 4:

1. **TrajViT2**: a video transformer encoder trained from scratch under the CLIP objective, where the tokenizer directly proposes trajectory tokens from video pixels.
2. **TrajAdapter**: a plug-in feature adapter that aggregates dense feature maps from any pretrained video encoder, using trajectory-based grouping to yield more informative representations for downstream probing tasks.
3. **TrajVLM**: a LLaVA-style [39] video–language model in which TrajTok serves as a connector between a ViT and an LLM, grouping ViT features along trajectories and passing the grouped trajectory tokens as visual inputs to the language model.

Tokenizer architecture. We use ConvNext-tiny [42] as the architecture for patch encoder. The perceiver modules in segmenter and trajectory encoder both have 2 layers and 8 attention heads. We use 128 learnable queries inside segmenter to cluster visual inputs into trajectories. Ablations of these design choices are presented in Section 5.

Pretraining the segmenter. When using TrajTok in pre-training task where the training data is fully controllable, we initialize the segmenter from scratch and jointly train the tokenizer with other modules using an added segmentation loss. However, when using the tokenizer as a feature adaptor in downstream tasks, we do not assume access to large-scale labeled segmentation data. We therefore pretrain a universal segmenter that can be reused across tasks without segmentation supervision during adaptation. To achieve this, we annotate 8M videos [11] and 15M images [9, 59] with panoptic object trajectory masks generated by the TrajViT pipeline, which serve as pseudo ground truth. Optimization details are described in the supplementary material. *This trained segmenter is reused in both TrajAdapter and TrajVLM.*

4.1. TrajViT2: A new video encoder

We first consider the scenario where the tokenizer operates directly on raw visual inputs and the resulting trajectory tokens serve as input tokens for a transformer video encoder—identical to the setup used in TrajViT. We named the trained encoder **TrajViT2**. Following the same protocol, we jointly train our tokenizer and a large transformer encoder from scratch under the CLIP objective on a large-scale captioning corpus. Unlike TrajViT, which relies on an external pipeline to generate trajectories, our model learns them end-to-end by training the segmenter simultaneously with the transformer, with an additional segmentation supervision.

Baselines. We compare TrajViT2 with several repre-

sentative architectures: (1) **ViT3D**, a standard video vision transformer that tokenizes inputs into fixed $16 \times 16 \times 2$ space–time patches; (2) **ViViT** [1], a factorized video transformer that decouples spatial and temporal attention for efficient video modeling; (3) **TokenLearner** [58], which dynamically learns a compact set of informative tokens via learned attention pooling; and (4) **Run Length Tokenization (RLT)** [14], a token-merging approach that aggregates redundant patches based on similarity of patch pixels. All baseline models follow their original token number settings.

Training and evaluation setup. We train all models with visual-text contrastive learning objective (CLIP loss) from scratch. All models adopt the same size transformer as in ViT-Large. Training corpus contains 4M video clips randomly sampled from Panda-70M [11] and 15M image–caption pairs from CC3M [9] and CC12M [59]. During training, we uniformly sample 8 frames per video, while in evaluation we uniformly sample 16 frames. We use a global batch size of 1024 images and 128 videos for 20 epochs on 8 A100 GPUs. After pretraining, all encoders are frozen and evaluated on a broad set of visual understanding benchmarks spanning both video and image domains: Video-text retrieval is evaluated on ActivityNet [8], VATEX [71], MSR-VTT [75], and Charades [60]; image-text retrieval is measured on COCO [37] and Flickr30K [52]; For image and video classification, we perform linear probing on Kinetics-400 (K400) [28], Something-Something V2 (SSV2) [23], ImageNet-1K (IN-1K) [18], CIFAR-100 [32], and Caltech-101 [20].

TrajViT2 performs better than all baselines. As shown in Table 1 and Table 2, TrajViT2 achieves consistent improvements over TrajViT and outperforms all baselines across both retrieval and classification benchmarks. Compared with TrajViT, it attains higher recall on all retrieval datasets (e.g., +4.1% vid2txt R@5 on ActivityNet and +4.0% on VATEX) and stronger accuracy on video and image classification tasks (e.g., +3.8% on K400 and +3.0% on SSV2). On ImageNet, however, TrajViT2 performs slightly lower than ViT3D. This is likely because ImageNet images typically contain a single centered foreground object and simple background, causing the segmenter to produce too few segments and therefore fewer tokens, which limits fine-grained discrimination on such easy scenes. Despite this, TrajViT2 matches or surpasses all other baselines on cross-domain and multi-object datasets, underscoring the strength of its trajectory-level tokenization.

TrajViT2 scales better. A key limitation of TrajViT lies in its scalability: its performance gain over ViT3D diminishes substantially as the pretraining dataset size increases from 1M to 8M samples. To examine the data-scaling behavior of TrajViT2, we follow the same experimental protocol used in TrajViT by partitioning the Panda-10M dataset into three random subsets containing 1M, 4M, and 8M video

Model	ActivityNet [8]		VATEX [71]		MSR-VTT [75]		Charades [60]		COCO [37]		Flickr30K [52]	
	txt2vid	vid2txt	txt2vid	vid2txt	txt2vid	vid2txt	txt2vid	vid2txt	txt2img	img2txt	txt2img	img2txt
ViT3D	37.1	35.6	36.4	60.2	31.4	58.1	13.8	12.9	61.5	67.4	75.2	83.6
TokenLearner	36.4	36.2	34.3	58.8	30.2	57.6	12.0	12.5	59.3	65.8	73.0	81.0
ViViT	33.9	33.2	34.0	57.6	29.6	55.2	12.3	11.8	57.8	64.1	71.6	79.3
RLT	35.9	35.0	35.0	58.4	30.5	57.1	12.2	12.3	59.6	66.1	72.8	81.2
TrajViT	38.4	38.1	36.0	61.1	31.6	61.2	14.7	14.6	63.2	69.0	77.4	85.1
TrajViT-2	40.1	42.2	37.9	65.0	33.2	65.3	15.9	16.5	68.1	75.6	83.5	90.4

Table 1. **Zero-shot video & image retrieval performance (R@5)**. TrajViT2 consistently surpasses all baselines by a large margin.

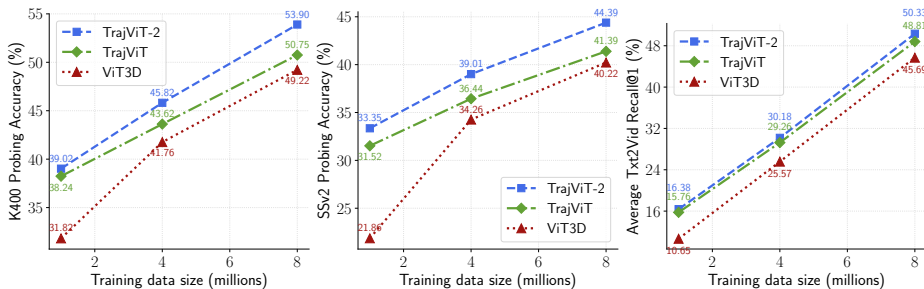


Figure 5. **Scaling with video training data**. TrajViT2 exhibits stronger scaling behavior than TrajViT and sustains a consistent performance margin over ViT3D at every data scale.

clips. We train TrajViT2, TrajViT, and ViT3D on all three scales and report their performance on video benchmarks. As shown in Figure 5, TrajViT2 exhibits a much stronger scaling trend than TrajViT. At the largest scale, TrajViT2 continues to outperform ViT3D by a large margin across both classification and retrieval tasks. We attribute this improvement to the end-to-end differentiability of TrajViT2’s tokenizer: the segmenter can flexibly adjust its segmentation behavior in response to the pretraining objective, rather than relying on fixed, heuristic segmentations. We give qualitative illustration in Figure 3.

TrajViT2 is highly efficient. Another drawback of TrajViT is its heavy computational overhead, caused by dependence on an external pipeline. TrajViT2 resolves this issue by replacing it with a lightweight, fully integrated segmenter. Our entire trajectory tokenizer contains only 46M parameters—an order of magnitude smaller compared to the 304M parameters of the ViT-Large backbone. We further compare inference FLOPs across input frame counts from 16 to 128 in Figure 6. TrajViT2 achieves nearly the same computational cost as the most efficient baseline, ViViT, in stark contrast to the quadratic scaling of patch-based ViT3D and the high-slope linear scaling of TrajViT. These results demonstrate that TrajViT2 achieves superior efficiency while maintaining strong performance.

4.2. TrajAdapter: A new video probing head

In practice, as pretrained large vision encoders continue to improve, it becomes increasingly desirable to directly reuse their output feature maps—often dense patch-level to-

Model	K400 [28]	SSv2 [23]	IN-1K [18]	CIFAR-100 [32]	Caltech-101 [20]
ViT3D	54.2	46.3	69.4	52.1	88.2
TokenLearner	52.9	42.4	67.3	49.5	86.7
ViViT	51.2	43.1	66.8	48.2	86.3
RLT	52.5	43.6	67.0	49.0	86.5
TrajViT	55.3	45.7	68.1	50.8	87.4
TrajViT-2	59.1	48.7	67.2	52.6	88.5

Table 2. **Action & image classification (attentive probe, top-1)**. IN-1K stands for ImageNet-1K. TrajViT2 improves upon TrajViT and outperforms all baselines in most of the benchmarks.

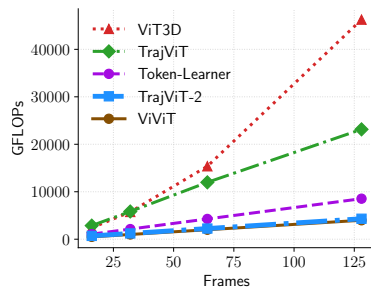


Figure 6. **Test time FLOPs comparison under different frame numbers**.

Probing Method	VideoMAE-v2 [68]		V-JEPA2 [2]	
	K400 [28]	SSv2 [23]	K400 [28]	SSv2 [23]
Linear probing	79.4	59.1	84.5	73.7
Attentive probing	80.2	59.7	85.1	74.2
Perceiver probing	79.9	59.8	84.7	74.2
TrajAdapter (1 token/traj)	82.0	60.4	87.2	74.6
TrajAdapter (2 token/traj)	82.4	60.8	87.8	74.9
TrajAdapter (4 token/traj)	82.5	60.9	88.0	75.1

Table 3. **Probing results on different video backbones**. Top-1 accuracy (%) on Kinetics-400 (K400) and Something-Something-V2 (SSv2) using various probing strategies. TrajAdapter consistently improves the downstream probing accuracy of pretrained backbone features, and performance further increases with more tokens per trajectory.

kens—for downstream tasks. We show that TrajTok can be directly plugged in as a lightweight adapter module to reorganize these dense feature maps into a compact set of trajectory tokens. We show this design not only reduces token number for downstream models but also provides a cost-effective way to enhance the probing performance of in downstream tasks without full fine-tuning.

Training and evaluation setup. We take video action classification as an example to demonstrate this setting. As illustrated in the second part of Figure 4, TrajTok is inserted after a frozen ViT backbone to reorganize output tokens, which are then used by an attentive probing head to predict classification logits. The segmenter is pretrained and *kept frozen* during probing, while the trajectory encoder is trained jointly with the probing head. For pretrained backbones, we adopt VideoMAE-v2 [68] and V-JEPA-2 [2], both using their ViT-Huge variants. We evaluate action



Figure 7. **Trajectory masks produced by our segmenter vs. by TrajViT pipeline.** While our segmenter produces coarser masks and may miss very small objects, it demonstrates strong semantic grouping ability that is sufficient for downstream understanding tasks.

recognition accuracy on the Kinetics-400 and Something-Something V2 (SSv2) benchmarks. Videos are uniformly sampled to 16 frames and sent to segmenter in one forward pass, producing a maximum of 128 trajectory tokens.

We compare our approach against three baselines: (1) naive linear probing, (2) attentive probing without adaptation, and (3) a Perceiver module of identical size and number of learnable queries as our trajectory encoder but without trajectory priors. In addition, we enable the adaptive token number mechanism in the trajectory encoder and report results for varying numbers of tokens per trajectory.

Results. Table 3 summarizes the top-1 classification accuracy of different probing strategies. Compared to both linear and attentive probing, TrajAdapter consistently achieves higher accuracy across datasets. Furthermore, our method outperforms the Perceiver-only variant, indicating that the improvement arises not merely from additional parameters but from the incorporation of trajectory priors. In fact, naively inserting a Perceiver module does not yield any gain over the attentive probing baseline. We also observe a steady performance increase as the token number per trajectory grows, even though the single-token configuration already surpasses conventional probing methods. These results demonstrate that the proposed tokenizer is not only effective for end-to-end video representation learning, but also serves as a plug-in adapter that enhances features in pretrained ViT backbones in a parameter-efficient manner.

4.3. TrajVLM: A new video-language model

Finally, we demonstrate that TrajTok can also serve as a connector between a vision encoder and a language model, providing an object-centric alternative to the patch-pooling connectors commonly used in large vision-language models (VLMs) [17, 25, 39, 54]. To this end, we build a small-scale model named **TrajVLM** by integrating our tokenizer into a standard LLaVA-style architecture (Figure 4 part 3). The goal of this experiment is not to compete with state-of-the-art VLMs, but rather to provide an *apple-to-apple* comparison between two connector designs: TrajTok and commonly-used patch pooling. Scaling TrajVLM to larger models with increased compute remains a future direction.

Architecture and Baseline. We use **Qwen3-4B** [78] as the

language model backbone and **SigLIP2-Huge** [65] as the vision encoder. For the baseline connector, we follow the design of **Molmo** [17], which employs per-frame, patch-based attention pooling. Specifically, each $x \times x$ spatial patch window is pooled into a single vector via a multi-head attention layer, where the mean patch embedding serves as the query. Notably, similar patch-pooling strategies are widely used in many of today’s most widely-used open-source vision-language models [54, 69, 76].

Training Data and Recipe. We adopt a subset of Molmo-2’s training corpus [16], including the PixMo captioning split, synthetic VideoQA split, and academic QA datasets (details in supplementary). Training follows Molmo’s two-stage procedure:

- **Pretraining.** All parameters are pretrained on the PixMo captioning split for one epoch to align visual features with the language model.
- **Fine-tuning.** The model is then fine-tuned for 10,000 steps on the remaining QA datasets.

All experiments are conducted on 8 A100 GPUs with a sequence length of 8,192 tokens. For TrajVLM frame sampling, we uniformly sample 128 video frames during both training and evaluation. TrajTok connector processes 128 frames by truncating them into 16-frame clips, each proposing a maximum of 128 tokens. For baseline PatchVLM, we train two versions of the model: a version that uses common patch pooling size $x = 3$, but can only support 32 frames due to sequence length limits; Another version that uses patch pool size $x = 9$ so that it can support 128-frame during training and the resulting number of visual tokens roughly matches that of our trajectory tokenizer, ensuring a fair comparison.

Results. We evaluate VLMs in common video QA benchmarks [21, 35, 41, 46, 47, 51, 70, 74, 83, 85]. Figure 8 shows that TrajVLM consistently outperforms the patch-pooling baselines on long-video benchmarks, including a notable +8.8% on LongVideoBench and +5.4% on LVBench over PatchVLM with default poolsize=3. We attribute our improvement to the fact that TrajTok produces semantically structured tokens that better support long-range reasoning while reducing redundancy. Notably, increasing the pooling window size in PatchVLM does not improve long-video performance on most benchmarks,

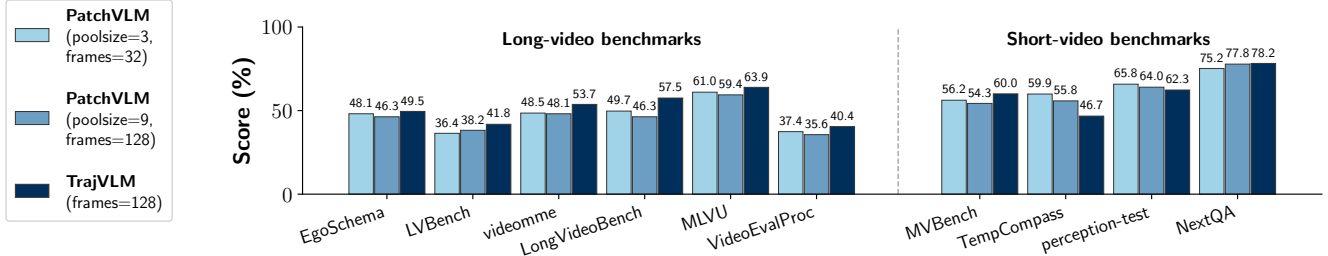


Figure 8. **VideoQA results for TrajTok applying to large vision-language model.** VLM with TrajTok as connector (TrajVLM) notably outperforms patch pooling baseline (PatchVLM) in long-video benchmarks, while the performance is mixed for short-video benchmark.

Module	Variation	VEQ (%)	STQ (%)	Retrieval (R@5)
Default Architecture		42.3	70.1	22.1
Backbone	no hierarchical features	39.3 (↓ 3.0)	66.2 (↓ 3.9)	19.2 (↓ 2.9)
Output Res.	56→224	44.1 (↑ 1.8)	73.0 (↑ 2.9)	22.0 (↓ 0.1)
Perceiver	no detach gradient	34.1 (↓ 8.2)	59.3 (↓ 10.8)	18.3 (↓ 3.8)
Seg. Loss	- dice loss	39.0 (↓ 3.3)	68.9 (↓ 1.2)	16.7 (↓ 5.4)
Seg. Loss	- focal loss	41.2 (↓ 1.1)	67.4 (↓ 2.7)	22.1 (0.0)
Seg. Loss	+ cross-entropy loss	42.1 (↓ 0.2)	71.3 (↑ 1.2)	21.3 (↓ 0.8)

Table 4. **Ablations of segmenter design.**

Module	Variation	1 token/traj	2 token/traj	4 token/traj
Default Architecture		22.1	23.0	23.2
Attention Mask	w/o mask	17.4 (↓ 4.7)	17.9 (↓ 5.1)	18.3 (↓ 4.9)
Query Init.	Fourier → random	22.1 (0.0)	22.5 (↓ 0.5)	21.9 (↓ 1.3)
Perceiver Depth	2 → 4	22.3 (↑ 0.2)	22.9 (↓ 0.1)	23.5 (↑ 0.3)

Table 5. **Ablations of trajectory encoder design.**

indicating that naively trading off spatial resolution with temporal support is insufficient for long-range reasoning. For Short-video benchmarks, we observe increased performance on [35, 74] but decreased performance on [41, 51]. Overall, these results validate TrajTok as an effective connector for VLMs, particularly in long-video understanding.

5. Ablating TrajTok design

We ablate the design choices of TrajTok under TrajViT2 setting, which trains a video encoder jointly optimized by the segmentation loss and CLIP loss. All experiments are trained on 1M video-caption pairs randomly sampled from Panda-10M for 10 epochs using 4 GPUs.

Ablation of segmenter design. We ablate the major design choices of the segmenter, including backbone hierarchy, gradient detachment, output resolution, and segmentation loss functions. We use VEQ and STQ metrics to quantify video panoptic segmentation quality following [81], and use average txt2vid R@5 accuracy across video retrieval benchmarks [8, 60, 71, 75] to quantify video understanding performance. As summarized in Table 4, removing hierarchical features yields consistent drops across VEQ, STQ, and retrieval accuracy, confirming the importance of multi-scale representations. Removing the gradient detachment of the patch-feature inside the perceiver causes large declines in segmentation quality due to coupled updates be-

tween queries and patch features. Increasing the output resolution slightly improves VEQ/STQ, but has negligible impact on retrieval, indicating that coarse masks are sufficient for semantic grouping. Among loss components, dice loss is the most critical: removing it severely harms both segmentation and understanding performance.

Ablation of trajectory encoder design. We also ablate the key components of the trajectory encoder, including the use of attention masks, query initialization strategies, and perceiver depth under the same retrieval task (Table 5). Removing the hard attention mask significantly degrades performance by weakening the association between trajectory tokens and their assigned regions. For query initialization under multi-token per trajectory setting, increasing the number of tokens per trajectory would not improve performance if Fourier-based query initialization is replaced by random initialization. That might be because different slots might extract the same trajectory information without explicit diversity encouragement. Finally, increasing perceiver depth yields only marginal improvements at higher computational cost, suggesting that a shallow perceiver is already sufficient for capturing local dynamics within trajectories.

6. Conclusion

We introduce TrajTok, an end-to-end and efficient tokenizer that learns to group visual trajectories and produce trajectory-level tokens directly from video inputs. Our experiments show that TrajTok is high-performance and highly versatile—it improves performance in three scenarios of pretraining video encoder, probing pretrained features, and training a video-language model. These results highlight the potential of trajectory-based tokenization as a more efficient and semantically aligned alternative to traditional patchification.

TrajTok: Learning Trajectory Tokens Enhances Video Understanding

Supplementary Material

7. Segementer Training Details

In the **TrajAdapter** and **TrajVLM** settings, we pretrain the trajectory segmenter once and reuse its weights for initialization during downstream probing and VLM training. This section provides full details of the dataset construction, annotation pipeline, filtering criteria, and training configuration for our segmenter training.

7.1. Dataset Construction

Sources. We construct a video & image corpus for segmenter training by combining: Panda (video) [11], CC12M (image) [9], CC3M (image) [59], and a subset of DataComp-50M (image) [22]. All samples are annotated with pseudo panoptic trajectory masks using the TrajViT trajectory-generation pipeline, followed with data filtering. We describe the details below.

Annotation Pipeline. We adopt the same annotation process as in the TrajViT paper [84]. In summary, the pipeline consists of four steps.

1. sample frames and detect keyframes based on feature changes in colorspace and Luminance Histogram.
2. generate panoptic object masks in the key frames using DirectSAM [10] model.
3. track objects across frames via SAM2 [57].
4. merge instance masks between CLIPs using heuristics like IOU overlaps to form long-term trajectories.

The pipeline uses external models like DirectSAM and SAM2 [10, 57]. For images, only spatial segmentation steps are applied.

Quality Filtering. We apply two filtering criteria to remove low-quality pseudo labels:

- **Coverage filter:** remove samples where the union of all trajectory masks covers less than 80% of pixels.
- **Object-count filter:** remove samples containing fewer than 10 detected objects.

After filtering, we retain roughly 2.5M images and 2.0M videos for segmenter pretraining.

7.2. Training Configuration

The segmenter is trained on the filtered dataset. Different from TrajViT2 where all modules are trained from scratch, we initialize the ConvNext-small patch encoder from DI-NOv3’s weights, which helps in the generalization performance of produced segments. Other modules are initialized from scratch. We train the model for 20 epochs with 8 A100 GPUs. We use the base learning rate of 1×10^{-3} , and adopt a linear decay learning-rate schedule with warm-up. Additional hyperparameters are summarized in Table 6.

Hyperparameter	Value
Resolution	224
Frame sampling	uniform 16 frames (videos only)
Optimizer	AdamW
Base LR	1×10^{-3}
Weight decay	0.01
Optimizer momentum	$\beta_1 = 0.9, \beta_2 = 0.999$
Batch size	video-128, image-512
Training epochs	20
LR schedule	linear decay
Warm up epochs	1
Warm up schedule	linear warm-up
Random crop scale	(0.2, 1.0)
Random crop ratio	(3/4, 4/3)
Horizontal flip probability	0.5
Color jitter probability	0.8
Gaussian blur probability	0.5
Grayscale probability	0.2

Table 6. Hyperparameters used for segmenter pretraining.

8. More Qualitative Examples of the Segmenter

We show examples of generated trajectories from our training set in Fig. 9. Overall, the segmenter exhibits strong semantic grouping ability, consistently discovering object-level regions that are sufficiently accurate for downstream understanding tasks. From the perspective of pixel-level segmentation quality, however, the lightweight design and low output resolution introduce several expected limitations: the model occasionally misses very small objects, may over-merge background regions, and produces imprecise object boundaries. These imperfections, while noticeable visually, do not hinder its effectiveness as a trajectory proposal module, as our downstream tasks primarily rely on correct semantic grouping rather than pixel-perfect masks.

9. Quantitative Evaluation of the Segmenter

Although the proposed segmenter in the main paper is intentionally lightweight—prioritizing semantic grouping over pixel-level precision—we additionally study how well it can perform on the standard panoptic video segmentation task when its capacity is scaled up. This experiment is conducted purely for analysis and is *not* used by any model in the main paper.

Scaling up the segmenter. We keep the same training dataset as described in Sec. 7.1, but increase the segmenter capacity in two ways: (1) replacing the ConvNeXt-Tiny patch encoder with a ConvNeXt-Large backbone and ex-

10. Training Details for TrajViT2

For all TrajViT2 experiments and baseline models, we optimize using the AdamW optimizer [45] with a base learning rate of 10^{-4} , weight decay of 10^{-2} , and mixed-precision training. We use a cosine annealing schedule with a linear warm-up of one epoch. The contrastive batch size is 128 for video clips and 1024 for images. All models are trained for 20 epochs using 8 NVIDIA A100 GPUs. During training, we apply standard video augmentation including random ColorJitter, Grayscale, Gaussian blur, horizontal flip, and resized cropping. At evaluation, we use only a single resizing operation for consistency. All models adopt a ViT-Large transformer and operate on 224-resolution inputs with 16 uniformly sampled frames.

11. Training Details for TrajAdapter

For all TrajAdapter experiments, we follow the standard protocol for probing pretrained video encoders. We use the AdamW optimizer with a learning rate of 1×10^{-4} and weight decay of 0.5. The pretrained backbone is kept frozen, while the trajectory encoder and probing head are updated. Before classification, video features are layer-normalized. We train with a batch size of 128 for 10 epochs. This configuration is used for all TrajAdapter experiments on both Kinetics-400 and Something-Something-V2 probing tasks.

12. Training Details for TrajVLM

We provide more training details for TrajVLM in this section.

Data sources. As discussed in the main paper, TrajVLM is trained using a two-stage procedure. For the pretraining stage, we closely follow the Molmo training paradigm [17] and use the same PixMo captioning split to align visual representations with the language model. For the instruction-tuning stage, we adopt the mixture of public academic VideoQA datasets and synthetic QA pairs curated in Molmo-2 [16]. These datasets span a wide range of reasoning skills—including temporal grounding, causal inference, long-horizon understanding, and multi-step procedural reasoning—and are summarized in Table 8. In total, the mixture contains approximately 5 million training examples.

Training hyperparameters. The training hyperparameters of the first stage follows Molmo [17]. We summarize the training hyperparameters for the second stage at Table 9.

References

[1] Anurag Arnab, Mostafa Dehghani, Georg Heigold, Chen Sun, Mario Lučić, and Cordelia Schmid. Vivit: A video vision transformer. In *ICCV*, 2021. 1, 2, 5

Table 8. **Datasets used for training TrajVLM under the “final” mixture.** This mixture combines a large set of academic VideoQA datasets, temporal reasoning datasets, and synthetic captioning/QA corpora.

Category	Dataset Name(s)	Notes / Source
Academic VideoQA	llava_video_mc_academic	MC-style QA
	llava_video_oe_academic	Open-ended QA
	cleverer	Causal & counterfactual reasoning
	funqa	Fine-grained temporal QA
	star	Long-horizon procedural QA
	intent_qa	Human intent reasoning
	tgif	Action/state transition QA
	video_localized_narratives	Localized narrations
	road_text_vqa	Driving VQA
	countix_oe	Counting QA (open-ended)
camerabench_qa	Camera-motion VQA	
Action / Activity QA	nextqa_mc	Next-QA multiple-choice
	news_video_qa_filtered	News comprehension QA
	how2qa	How-to instructional QA
	sutd_trafficqa	Traffic event QA
	social_lig2	Social reasoning
	sportsqa_oe	Sports QA (OE)
	cinepile	Movie understanding QA
	ssv2_qa	Something-Something QA
	moments_in_time_qa	Activity recognition QA
	kinetics_qa	Kinetics QA
charades_sta_all_qa	Charades Spatial-Temporal QA	
coin_all_qa	Procedural task step QA	
Video Captioning / Highlighting	youcook2_all_qa	Recipe video QA/caption
	activitynet_all_qa	ActivityNet QA/caption
	ego4d_all	Ego4D narrations + QA
	video_localized_narratives_caption	Captioning corpus
	qv_highlights	Highlight detection w/ text
	motionbench_train	Long-range motion reasoning
Internal / Synthetic VideoQA	vixmo_syn_video_capqa_v2	200K synthetic QA pairs
	vixmo3_top_level_captions_min_3	101K curated human captions
	vixmo_clip_qa_all	CLIP-constructed QA corpora

Hyperparameter	Value
Max video frames	128
Total training steps	10,000
Training stages	Pretraining + Instruction tuning
Sequence length	8192
Global batch size	32
Device batch size	4
Number of GPUs	8 × A100 (80GB)
Precision	bfloat16 (AMP)
Optimizer	AdamW
LLM learning rate	1×10^{-5}
ViT learning rate	5×10^{-6}
Connector learning rate	5×10^{-6}
Learning rate warmup	200 steps
LR schedule	Multimodal cosine decay
Weight decay	0.0 (LLM / ViT / connector)
Adam momentum	$\beta_1 = 0.9, \beta_2 = 0.95$
Adam ϵ	1×10^{-6}
Gradient clipping	1.0

Table 9. **Key hyperparameters used for training TrajVLM.** Values reflect the shared configuration across all VLM experiments.

[2] Mido Assran, Adrien Bardes, David Fan, et al. V-jepa 2: Self-supervised video models enable understanding, prediction and planning. *arXiv preprint arXiv:2506.09985*, 2025. 1, 6

[3] Adrien Bardes, Quentin Garrido, Jean Ponce, Xinlei Chen, Michael Rabbat, Yann LeCun, Mahmoud Assran, and Nicolas Ballas. V-jepa: Video joint-embedding predictive architecture. *arXiv preprint arXiv:2404.08471*, 2024. 1

[4] Gedas Bertasius, Heng Wang, and Lorenzo Torresani. Is

- space-time attention all you need for video understanding? In *ICML*, 2021. 1, 2
- [5] Lukas Beyer, Xiaohua Zhai, Alexander Kolesnikov, Joan Puigcerver, Alexander Steiner, Daniel Keysers, Barret Zoph, and Neil Houlsby. Flexivit: One model for all patch sizes. In *CVPR*, 2023. 1
- [6] Daniel Bolya, Cheng-Yang Fu, Xiaoliang Dai, Peizhao Zhang, Christoph Feichtenhofer, and Judy Hoffman. Token merging: Your vit but faster. In *ICLR*, 2023. 1, 2
- [7] Chris Burgess, Hyunjik Kim, Loic Matthey, Nick Waters, Rishabh Kabra, Irina Higgins, Matthew Botvinick, and Alexander Lerchner. Monet: Unsupervised scene decomposition and representation. In *arXiv:1901.11390*, 2019. 2
- [8] Fabian Caba Heilbron, Victor Escorcia, Bernard Ghanem, and Juan Carlos Niebles. Activitynet: A large-scale video benchmark for human activity understanding. In *Proceedings of the IEEE Conference on Computer Vision and Pattern Recognition (CVPR)*, 2015. 5, 6, 8
- [9] Soravit Changpinyo, Piyush Sharma, Nan Ding, and Radu Soricut. Conceptual 12m: Pushing web-scale image-text pre-training to recognize long-tail visual concepts. In *Proceedings of the IEEE/CVF conference on computer vision and pattern recognition*, pages 3558–3568, 2021. 5, 9
- [10] Delong Chen, Samuel Cahyawijaya, Jianfeng Liu, Baoyuan Wang, and Pascale Fung. Subobject-level image tokenization. *arXiv preprint arXiv:2402.14327*, 2024. 2, 9
- [11] Tsai-Shien Chen, Aliaksandr Siarohin, Willi Menapace, Ekaterina Deyneka, Hsiang-wei Chao, Byung Eun Jeon, Yuwei Fang, Hsin-Ying Lee, Jian Ren, Ming-Hsuan Yang, et al. Panda-70m: Captioning 70m videos with multiple cross-modality teachers. In *Proceedings of the IEEE/CVF Conference on Computer Vision and Pattern Recognition*, pages 13320–13331, 2024. 5, 9
- [12] Bowen Cheng, Ishan Misra, Alexander G Schwing, Alexander Kirillov, and Rohit Girdhar. Masked-attention mask transformer for universal image segmentation. In *Proceedings of the IEEE/CVF conference on computer vision and pattern recognition*, pages 1290–1299, 2022. 2, 3
- [13] Joonmyung Choi, Sanghyeok Lee, Jaewon Chu, Minhyuk Choi, and Hyunwoo J. Kim. vid-tldr: Training free token merging for light-weight video transformer. In *CVPR*, 2024. 2
- [14] Rohan Choudhury, Guanglei Zhu, Sihan Liu, Koichiro Niinuma, Kris M. Kitani, and László A. Jeni. Don’t look twice: Faster video transformers with run-length tokenization. In *NeurIPS*, 2024. 1, 2, 5
- [15] Rohan Choudhury, JungEun Kim, Jinhung Park, Eunho Yang, László A. Jeni, and Kris M. Kitani. Accelerating vision transformers with adaptive patch sizes. *arXiv preprint arXiv:2510.18091*, 2025. 1, 2
- [16] Christopher Clark, Jieyu Zhang, Zixian Ma, Jae Sung Park, Rohun Tripathi, Sangho Lee, Mohammadreza Salehi, Jason Ren, Chris Dongjoo Kim, Yinuo Yang, Vincent Shao, Yue Yang, Weikai Huang, Ziqi Gao, Taira Anderson, Jianrui Zhang, Jitesh Jain, George Stoica, Ali Farhadi, and Ranjay Krishna. Molmo 2: Open weights and open data for state-of-the-art video and image models, 2026. arXiv:2601.10611. 7, 11
- [17] Matt Deitke, Christopher Clark, Sangho Lee, Rohun Tripathi, Yue Yang, et al. Molmo and pixmo: Open weights and open data for state-of-the-art vision-language models. *arXiv preprint arXiv:2409.17146*, 2024. 1, 7, 11
- [18] Jia Deng, Wei Dong, Richard Socher, Li-Jia Li, Kai Li, and Li Fei-Fei. Imagenet: A large-scale hierarchical image database. In *Proceedings of the IEEE Conference on Computer Vision and Pattern Recognition (CVPR)*, 2009. 5, 6
- [19] Mohsen Fayyaz, Soroush Abbasi Koohpayegani, and Jürgen Gall. Adaptive token sampling for efficient vision transformers. In *ECCV*, 2022. 2
- [20] Li Fei-Fei, Rob Fergus, and Pietro Perona. Learning generative visual models from few training examples: An incremental bayesian approach tested on 101 object categories. In *IEEE Conference on Computer Vision and Pattern Recognition Workshop (CVPRW)*, 2004. 5, 6
- [21] Chaoyou Fu et al. Video-mme: A comprehensive evaluation benchmark of multi-modal llms in video analysis. *arXiv:2405.21075*, 2024. 7
- [22] Samir Yitzhak Gadre, Gabriel Ilharco, Alex Fang, Jonathan Hayase, Georgios Smyrnis, Thao Nguyen, Ryan Marten, Mitchell Wortsman, Dhruva Ghosh, Jieyu Zhang, et al. Datcomp: In search of the next generation of multimodal datasets. *Advances in Neural Information Processing Systems*, 36:27092–27112, 2023. 9
- [23] Raghav Goyal, Samira Ebrahimi Kahou, Vincent Michalski, Joanna Materzynska, Sebastian Westphal, Heuna Kim, Valentin Haenel, Moritz Früh, Peter Yianilos, Marcel Mueller-Freitag, et al. The “something something” video database for learning and evaluating visual common sense. In *Proceedings of the IEEE International Conference on Computer Vision (ICCV)*, 2017. 5, 6
- [24] Klaus Greff, Raphael L Kaufman, and et al. Multi-object representation learning with iterative variational inference. In *ICML*, 2019. 2
- [25] Xiaohu Huang, Hao Zhou, and Kai Han. Prunevid: Visual token pruning for efficient video large language models. *arXiv preprint arXiv:2412.16117*, 2024. 2, 7
- [26] Andrew Jaegle et al. Perceiver: General perception with iterative attention. *ICML*, 2021. 2, 3
- [27] Andrew Jaegle et al. Perceiver io: A general architecture for structured inputs & outputs. *arXiv:2107.14795*, 2021. 2
- [28] Will Kay, Joao Carreira, Karen Simonyan, et al. The kinetics human action video dataset. In *arXiv preprint arXiv:1705.06950*, 2017. 5, 6
- [29] Minchul Kim et al. Token fusion: Bridging the gap between token pruning and token merging. In *WACV*, 2024. 2
- [30] Thomas Kipf, Gamaleldin F. Elsayed, Aravindh Mahendran, Austin Stone, Sara Sabour, Georg Heigold, Rico Jonchkowski, Alexey Dosovitskiy, and Klaus Greff. Conditional object-centric learning from video. In *ICLR*, 2022. 2
- [31] Alexander Kirillov, Eric Mintun, Nikhila Ravi, Hanzi Mao, Chloe Rolland, Laura Gustafson, Tete Xiao, Spencer Whitehead, Alexander C Berg, Wan-Yen Lo, et al. Segment anything. In *Proceedings of the IEEE/CVF international conference on computer vision*, pages 4015–4026, 2023. 2

- [32] Alex Krizhevsky. Learning multiple layers of features from tiny images. Technical report, University of Toronto, 2009. 5, 6
- [33] Pulkit Kumar, Shuaiyi Huang, Matthew Walmer, Sai Saketh Rambhatla, and Abhinav Shrivastava. Tokrens: Semantic-aware relational trajectory tokens for few-shot action recognition. In *Proceedings of the IEEE/CVF International Conference on Computer Vision*, pages 13544–13556, 2025. 2
- [34] Aditya Kusupati, Gantavya Bhatt, Aniket Rege, Matthew Wallingford, Aditya Sinha, Vivek Ramanujan, William Howard-Snyder, Kaifeng Chen, Sham Kakade, Prateek Jain, et al. Matryoshka representation learning. *Advances in Neural Information Processing Systems*, 35:30233–30249, 2022. 2, 4
- [35] Kunchang Li, Yali Wang, Yinan He, Yizhuo Li, Yi Wang, Yi Liu, Zun Wang, Jilan Xu, Guo Chen, Ping Luo, Limin Wang, and Yu Qiao. Mvbench: A comprehensive multimodal video understanding benchmark. In *Proceedings of the IEEE/CVF Conference on Computer Vision and Pattern Recognition (CVPR)*, 2024. 7, 8
- [36] Youwei Liang, Chongjian Ge, Zhan Tong, Yibing Song, and Jue Wang. Not all patches are what you need: Expediting vision transformers via token reorganizations. In *ICLR*, 2022. 2
- [37] Tsung-Yi Lin, Michael Maire, Serge Belongie, James Hays, Pietro Perona, Deva Ramanan, Piotr Dollár, and C. Lawrence Zitnick. Microsoft coco: Common objects in context. In *European Conference on Computer Vision (ECCV)*, 2014. 5, 6
- [38] Tsung-Yi Lin, Priya Goyal, Ross Girshick, Kaiming He, and Piotr Dollár. Focal loss for dense object detection. In *Proceedings of the IEEE international conference on computer vision*, pages 2980–2988, 2017. 4
- [39] Haotian Liu, Chunyuan Li, Qingyang Wu, and Yong Jae Lee. Visual instruction tuning. *Advances in neural information processing systems*, 36:34892–34916, 2023. 5, 7
- [40] Xiangrui Liu, Yan Shu, Zheng Liu, Ao Li, Yang Tian, and Bo Zhao. Video-xl-pro: Reconstructive token compression for extremely long video understanding. *arXiv preprint arXiv:2503.18478*, 2025. 2
- [41] Yutao Liu et al. Tempcompass: Do video llms really understand videos? In *Findings of the Association for Computational Linguistics (ACL)*, 2024. 7, 8
- [42] Zhuang Liu, Hanzi Mao, Chao-Yuan Wu, Christoph Feichtenhofer, Trevor Darrell, and Saining Xie. A convnet for the 2020s. In *Proceedings of the IEEE/CVF conference on computer vision and pattern recognition*, pages 11976–11986, 2022. 3, 5
- [43] Ze Liu, Jia Ning, Yue Cao, Yixuan Wei, Zheng Zhang, Stephen Lin, and Han Hu. Video swin transformer. In *CVPR*, 2022. 2
- [44] Francesco Locatello, Dirk Weissenborn, and et al. Object-centric learning with slot attention. In *NeurIPS*, 2020. 2
- [45] Ilya Loshchilov and Frank Hutter. Decoupled weight decay regularization. In *International Conference on Learning Representations (ICLR)*, 2019. 11
- [46] Wentao Ma, Weiming Ren, Yiming Jia, Zhuofeng Li, Ping Nie, Ge Zhang, and Wenhua Chen. Videoeval-pro: Robust and realistic long video understanding evaluation. *arXiv preprint arXiv:2505.14640*, 2025. 7
- [47] Karttikeya Mangalam, Raiymbek Akshulakov, and Jitendra Malik. Egoschema: A diagnostic benchmark for very long-form video language understanding. In *Advances in Neural Information Processing Systems (NeurIPS), Datasets and Benchmarks Track*, 2023. 7
- [48] Jieru Mei, Liang-Chieh Chen, Alan Yuille, and Cihang Xie. Spformer: Enhancing vision transformer with superpixel representation. *arXiv preprint arXiv:2401.02931*, 2024. 1
- [49] Jiaxu Miao, Xiaohan Wang, Yu Wu, Wei Li, Xu Zhang, Yunchao Wei, and Yi Yang. Large-scale video panoptic segmentation in the wild: A benchmark. In *Proceedings of the IEEE/CVF Conference on Computer Vision and Pattern Recognition*, pages 21033–21043, 2022. 10
- [50] Arsha Nagrani, Anurag Arnab, and Cordelia Schmid. Attention bottlenecks for multimodal fusion. In *NeurIPS*, 2021. 2
- [51] Viorica Pătrăucean, Lucas Smaira, Ankush Gupta, et al. Perception test: A diagnostic benchmark for multimodal video models. In *Advances in Neural Information Processing Systems (NeurIPS), Datasets and Benchmarks Track*, 2023. 7, 8
- [52] Bryan A. Plummer, Liwei Wang, Christopher Cervantes, Juan C. Caicedo, Julia Hockenmaier, and Svetlana Lazebnik. Flickr30k entities: Collecting region-to-phrase correspondences for richer image-to-sentence models. In *Proceedings of the IEEE International Conference on Computer Vision (ICCV)*, 2015. 5, 6
- [53] Zenon W. Pylyshyn and Roger W. Storm. Tracking multiple independent targets: Evidence for a parallel tracking mechanism. *Spatial Vision*, 3(3):179–197, 1988. 2
- [54] Qwen Team. Qwen2.5-vl technical report. *arXiv preprint arXiv:2502.13923*, 2025. 1, 7
- [55] Alec Radford, Jong Wook Kim, Chris Hallacy, Aditya Ramesh, Gabriel Goh, Sandhini Agarwal, Girish Sastry, Amanda Askell, Pamela Mishkin, Jack Clark, Gretchen Krueger, and Ilya Sutskever. Learning transferable visual models from natural language supervision. In *ICML*, 2021. 2
- [56] Yongming Rao, Wenliang Zhao, Benlin Liu, Jiwen Lu, Jie Zhou, and Cho-Jui Hsieh. Dynamicvit: Efficient vision transformers with dynamic token sparsification. In *NeurIPS*, 2021. 2
- [57] Nikhila Ravi et al. Sam 2: Segment anything in images and videos. *arXiv:2408.00714*, 2024. 2, 9, 10
- [58] Michael S. Ryoo, AJ Piergiovanni, Mingxing Tan, and Anelia Angelova. Tokenlearner: What can 8 learned tokens do for images and videos? *NeurIPS*, 2021. 1, 2, 5
- [59] Piyush Sharma, Nan Ding, Sebastian Goodman, and Radu Soricut. Conceptual captions: A cleaned, hypernymed, image alt-text dataset for automatic image captioning. In *Proceedings of the 56th Annual Meeting of the Association for Computational Linguistics (Volume 1: Long Papers)*, pages 2556–2565, 2018. 5, 9
- [60] Gunnar A. Sigurdsson, Gul Varol, Xiaolong Wang, Ali Farhadi, Ivan Laptev, and Abhinav Gupta. Hollywood in

- homes: Crowdsourcing data collection for activity understanding. In *Proceedings of the European Conference on Computer Vision (ECCV)*, 2016. 5, 6, 8
- [61] Satvik Singh, Chris Burgess, and Alexander Lerchner. Scaling slot attention for unsupervised object discovery. In *ICLR*, 2022. 2
- [62] Elizabeth S. Spelke. Principles of object perception. *Cognitive Science*, 14(1):29–56, 1990. 2
- [63] Jianlin Su, Murtadha Ahmed, Yu Lu, Shengfeng Pan, Wen Bo, and Yunfeng Liu. Roformer: Enhanced transformer with rotary position embedding. *Neurocomputing*, 568:127063, 2024. 3
- [64] Carole H Sudre, Wenqi Li, Tom Vercauteren, Sebastien Ourselin, and M Jorge Cardoso. Generalised dice overlap as a deep learning loss function for highly unbalanced segmentations. In *International Workshop on Deep Learning in Medical Image Analysis*, pages 240–248. Springer, 2017. 4
- [65] Michael Tschannen, Alexey Gritsenko, Xiao Wang, Muhammad Ferjad Naeem, Ibrahim Alabdulmohsin, Nikhil Parthasarathy, Talfan Evans, Lucas Beyer, Ye Xia, Basil Mustafa, et al. Siglip 2: Multilingual vision-language encoders with improved semantic understanding, localization, and dense features. *arXiv preprint arXiv:2502.14786*, 2025. 7
- [66] Johan Wagemans, James H. Elder, Michael Kubovy, Stephen E. Palmer, Irving Biederman, et al. A century of gestalt psychology in visual perception: I. perceptual grouping and figure–ground organization. *Psychological Bulletin*, 138(6):1172–1217, 2012. 2
- [67] Junke Wang et al. Efficient video transformers with spatial-temporal token selection. In *ECCV*, 2022. 2
- [68] Limin Wang, Bingkun Huang, Zhiyu Zhao, Zhan Tong, Yinan He, Yi Wang, Yali Wang, and Yu Qiao. Videomae v2: Scaling video masked autoencoders with dual masking. In *Proceedings of the IEEE/CVF conference on computer vision and pattern recognition*, pages 14549–14560, 2023. 6
- [69] Weiyun Wang, Zhangwei Gao, Lixin Gu, Hengjun Pu, Long Cui, Xingguang Wei, Zhaoyang Liu, Linglin Jing, Shenglong Ye, Jie Shao, et al. Internv1.3. 5: Advancing open-source multimodal models in versatility, reasoning, and efficiency. *arXiv preprint arXiv:2508.18265*, 2025. 7
- [70] Weihang Wang et al. Lvbench: An extreme long video understanding benchmark. *arXiv preprint arXiv:2406.08035*, 2024. 7
- [71] Xin Wang, Jiawei Wu, Junkun Chen, Lei Li, Yuan-Fang Wang, and William Yang Wang. Vatex: A large-scale, high-quality multilingual dataset for video-and-language research. In *Proceedings of the IEEE/CVF International Conference on Computer Vision (ICCV)*, 2019. 5, 6, 8
- [72] Yi Wang, Yinan He, Yizhuo Li, Kunchang Li, Jiashuo Yu, Xin Ma, et al. Internvid: A large-scale video-text dataset for multimodal understanding and generation. *arXiv preprint arXiv:2307.06942*, 2023. 1
- [73] Shiwei Wu, Joya Chen, Kevin Qinghong Lin, Qimeng Wang, Yan Gao, Qianli Xu, Tong Xu, Yao Hu, Enhong Chen, and Mike Zheng Shou. Videollm-mod: Efficient video-language streaming with mixture-of-depths vision computation. *arXiv preprint arXiv:2408.16730*, 2024. 2
- [74] Junbin Xiao, Xindi Shang, Angela Yao, and Tat-Seng Chua. Next-qa: Next phase of question-answering to explaining temporal actions. In *Proceedings of the IEEE/CVF Conference on Computer Vision and Pattern Recognition (CVPR)*, 2021. 7, 8
- [75] Jun Xu, Tao Mei, Ting Yao, and Yong Rui. Msr-vtt: A large video description dataset for bridging video and language. In *Proceedings of the IEEE Conference on Computer Vision and Pattern Recognition (CVPR)*, 2016. 5, 6, 8
- [76] Mingze Xu, Mingfei Gao, Zhe Gan, Hong-You Chen, Zhengfeng Lai, Haiming Gang, Kai Kang, and Afshin Dehghan. Slowfast-llava: A strong training-free baseline for video large language models. *arXiv preprint arXiv:2407.15841*, 2024. 7
- [77] Shilin Yan, Jiaming Han, Joey Tsai, Hongwei Xue, Rongyao Fang, Lingyi Hong, Ziyu Guo, and Ray Zhang. Crosslmm: Decoupling long video sequences from lmm via dual cross-attention mechanisms. *arXiv preprint arXiv:2505.17020*, 2025. 2
- [78] An Yang, Anfeng Li, Baosong Yang, Beichen Zhang, Binyuan Hui, Bo Zheng, Bowen Yu, Chang Gao, Chengen Huang, Chenxu Lv, et al. Qwen3 technical report. *arXiv preprint arXiv:2505.09388*, 2025. 7
- [79] Zongxin Yang, Yunchao Wei, and Yi Yang. Xmem: Long-term video object segmentation with an atkinson–shiffrin memory model. In *ECCV*, 2022. 2
- [80] Zongxin Yang et al. Efficient video object segmentation via decomposing attention with optimized memory. *arXiv preprint arXiv:2306.00961*, 2023. 2
- [81] Mingqiao Ye, Seoung Wug Oh, Lei Ke, and Joon-Young Lee. Entitysam: Segment everything in video. In *Proceedings of the Computer Vision and Pattern Recognition Conference*, pages 24234–24243, 2025. 3, 8, 10
- [82] Yuqian Yuan, Wentong Li, Jian Liu, Dongqi Tang, Xinjie Luo, Chi Qin, Lei Zhang, and Jianke Zhu. Osprey: Pixel understanding with visual instruction tuning. In *CVPR*, 2024. arXiv:2312.10032. 2
- [83] Hongjie Zhang et al. Lvbench: A benchmark for long-form video understanding. *arXiv preprint arXiv:2312.04817*, 2023. 7
- [84] Chenhao Zheng, Jieyu Zhang, Mohammadreza Salehi, Ziqi Gao, Vishnu Iyengar, Norimasa Kobori, Quan Kong, and Ranjay Krishna. One trajectory, one token: Grounded video tokenization via panoptic sub-object trajectory. *arXiv:2505.23617*, 2025. 1, 2, 4, 9
- [85] Junjie Zhou et al. Mlvu: Benchmarking multi-task long video understanding. In *Proceedings of the IEEE/CVF Conference on Computer Vision and Pattern Recognition (CVPR)*, 2025. 7